

Dual-wavelength pumped latticed Fermi-Pasta-Ulam recurrences in nonlinear Schrödinger equation

Qian Zhang(张倩), Xiankun Yao(姚献坤), and Heng Dong(董恒)

Citation: Chin. Phys. B, 2024, 33 (**3**): 030502. DOI: 10.1088/1674-1056/ad181e
Journal homepage: http://cpb.iphy.ac.cn; http://iopscience.iop.org/cpb

What follows is a list of articles you may be interested in

A lightweight symmetric image encryption cryptosystem in wavelet domain based on an improved sine map

Baichi Chen(陈柏池), Linqing Huang(黄林青), Shuting Cai(蔡述庭), Xiaoming Xiong(熊晓明), and Hui Zhang(张慧)

Chin. Phys. B, 2024, 33 (**3**): 030501. DOI: 10.1088/1674-1056/ad1030

Multiple mixed state variable incremental integration for reconstructing extreme multistability in a novel memristive hyperchaotic jerk system with multiple cubic nonlinearity

Meng-Jiao Wang(王梦蛟) and Lingfang Gu(辜玲芳)

Chin. Phys. B, 2024, 33 (**2**): 020504. DOI: 10.1088/1674-1056/acddd0

Modulational instability of a resonantly polariton condensate in discrete lattices

Wei Qi(漆伟), Xiao-Gang Guo(郭晓刚), Liang-Wei Dong(董亮伟), and Xiao-Fei Zhang(张晓斐)

Chin. Phys. B, 2023, 32 (**3**): 030502. DOI: 10.1088/1674-1056/ac891a

Controllable optical superregular breathers in the femtosecond regime

Yang Ren(任杨), Zhan-Ying Yang(杨战营), Chong Liu(刘冲), Wen-Li Yang(杨文力)

Chin. Phys. B, 2018, 27 (**1**): 010504. DOI: 10.1088/1674-1056/27/1/010504

Kuznetsov-Ma soliton and Akhmediev breather of higher-order nonlinear Schrödinger equation

Zai-Dong Li(李再东), Xuan Wu(吴璇), Qiu-Yan Li(李秋艳), P B He(贺鹏斌)

Chin. Phys. B, 2016, 25 (**1**): 010507. DOI: 10.1088/1674-1056/25/1/010507

Dual-wavelength pumped latticed Fermi–Pasta–Ulam recurrences in nonlinear Schrödinger equation

Qian Zhang(张倩)[1], Xiankun Yao(姚献坤)[1,2,3,†], and Heng Dong(董恒)[1]

[1] *School of Physics, Northwest University, Xi'an* 710127, *China*
[2] *Shaanxi Key Laboratory for Theoretical Physics Frontiers, Xi'an* 710127, *China*
[3] *Peng Huanwu Center for Fundamental Theory, Xi'an* 710127, *China*

(Received 16 October 2023; revised manuscript received 18 December 2023; accepted manuscript online 22 December 2023)

We show that the nonlinear stage of the dual-wavelength pumped modulation instability (MI) in nonlinear Schrödinger equation (NLSE) can be effectively analyzed by mode truncation methods. The resulting complicated heteroclinic structure of instability unveils all possible dynamic trajectories of nonlinear waves. Significantly, the latticed-Fermi–Pasta–Ulam recurrences on the modulated-wave background in NLSE are also investigated and their dynamic trajectories run along the Hamiltonian contours of the heteroclinic structure. It is demonstrated that there has much richer dynamic behavior, in contrast to the nonlinear waves reported before. This novel nonlinear wave promises to inject new vitality into the study of MI.

Keywords: modulation instability, dual-wavelength pumps, latticed-Fermi–Pasta–Ulam recurrences

PACS: 05.45.–a, 52.35.Mw **DOI:** 10.1088/1674-1056/ad181e

1. Introduction

In the past, modulation instability (MI) has been extensively studied in many areas including Bose–Einstein condensate,[1,2] hydrodynamics,[3] nonlinear fiber optics[4] and plasma physics,[5] etc. It is associated with the growth of perturbated on a continuous-wave background,[6] and is also the key mechanism in the development of a variety of complex patterns, such as Akhmediev breathers (ABs),[7–9] Fermi–Pasta–Ulam (FPU) recurrences,[10–12] superregular breathers,[13–15] Kuznetsov–Ma breathers,[16,17] and rogue waves.[18–21] Through linear stability analysis, MI in the initial stage reflects the exponential growth of the spectral sideband perturbation until MI enters a nonlinear stage when the growth reaches saturation, and the wave dynamics exhibit a complex frequency conversion process.[22,23] The multi-wave truncation method[24–27] (MWT) has been used to analyze the dynamics of MI in various systems, including birefringence fibers,[23,28] the dispersion-oscillating fibers,[29,30] the pure-quartic dispersion systems,[22] and the dissipative systems.[31–33] The method only considers the interaction between the pump and the first-order sidebands, and ignores the influence of the higher-order sidebands. The heteroclinic structure[34] (i.e., Hamiltonian contour line on the phase-space plane) obtained by the mode truncation method reveals all possible dynamic trajectories of nonlinear waves.

MI can exist not only on the aforementioned plane wave background, but also on the modulated-wave background.[35–37] Modulated wave is equivalently viewed as the superposition of two plane waves of different frequencies. In general, the coupled nonlinear Schrödinger equation (CNLSE) is used to describe the perturbation of dual-wavelength pumps case.[38] However, the MI of dual-wavelength pumps described in CNLSE does not intuitively reflect dual-wavelength characteristics, and some specific physical phenomena are lost by neglecting the four-wave mixing term in the process.

In this paper, we address this issue and comprehensively analyze the MI of dual-wavelength pumps by using NLSE with an approximate stationary solution, representing a modulated wave. Firstly, the linear stage of MI is analyzed by linear stability analysis. Subsequently, a complicated heteroclinic structure is obtained by the MWT method. We also show that different FPU recurrences are separated by separatrix on the heteroclinic structure. In addition, we report the occurrence of latticed-FPU patterns excited on the modulated-wave background in NLSE.

2. Physical model and linear stability analysis

The propagating dynamic of light is governed by the following dimensionless NLSE:

$$\mathrm{i}\frac{\partial \psi}{\partial z}+\frac{1}{2}\frac{\partial^2 \psi}{\partial t^2}+|\psi|^2\psi=0, \tag{1}$$

where ψ is the normalized field. z and t are normalized distance and time, respectively.

It is well known that the nonlinear process of energy exchange between four equidistant and symmetric frequency components of the field in NLSE can be solved exactly by Jacobi elliptic functions.[39] In this paper, when the frequency

†Corresponding author. E-mail: yaoxk@nwu.edu.cn

© 2024 Chinese Physical Society and IOP Publishing Ltd

difference of the dual-wavelength is large enough, it is feasible to approximate the elliptic-function solution as a cosine function, which is convenient and effective to analyze the MI of dual-wavelength. It reads

$$\psi_0(z,t) = \sqrt{2P}\cos(\omega_0 t)\exp[\mathrm{i}\varphi(z)], \tag{2}$$

in fact, it is an approximate stationary solution. P is the total power of two plane waves. The phase shift is given by $\varphi(z) = 0.5(3P-\omega_0^2)z$, where $\pm\omega_0$ denote the center frequency of the two plane waves. It is important to note that ω_0 should be large enough so that the two wavelength pumps are not located with each other's MI gain region (i.e., $\omega_0 > \pm(P)^{1/2}$). Figure 1(a) shows the stable transmission of Eq. (2) for the case $\omega_0 = 5$.

The stability of stationary solution is examined by inserting in Eq. (1) the ansatz $\psi = \sqrt{P/2}\exp(\mathrm{i}\omega_0 t + \mathrm{i}\varphi)(1+a_1) + \sqrt{P/2}\exp(-\mathrm{i}\omega_0 t + \mathrm{i}\varphi)(1+a_2)$, where a is a perturbation at modulational frequency ω and wavenumber K of the form $a_j = \{\varepsilon_{j1}\exp[\mathrm{i}(Kz-\omega t)] + \varepsilon_{j2}\exp[-\mathrm{i}(Kz-\omega t)]\}$ with $j = 1, 2$. Then, through linear stability analysis, we obtain the dispersion relation $K = \pm\omega[\omega_0^2 + (\omega^2/4) - (P/2) \pm (\omega^2\omega_0^2 - 2\omega_0^2 P + P^2)^{1/2}]^{1/2}$. The instability gain can be obtained by $g(\omega) = 2\mathrm{Im}(K)$. Figure 1(b) displays the MI gain spectrum (only the first branch is shown), where the gain exists only if $|\omega| < \omega_{\max} = [(2P-P^2)/\omega_0^2]^{1/2}$. Both the maximum gain value and the frequency range increase with an increase in the power P and pump frequency ω_0. When $\omega = [(P-0.5P^2)/\omega_0^2]^{1/2}$, the gain reaches the maximum, and the frequency domain diagram of the perturbation of the dual-wavelength pump is shown in Fig. 1(c). The theory result can be examined in the experiment by modulating the intensity of two CW lasers with different wavelengths and coupling them into a segment of optical fiber for transmission.

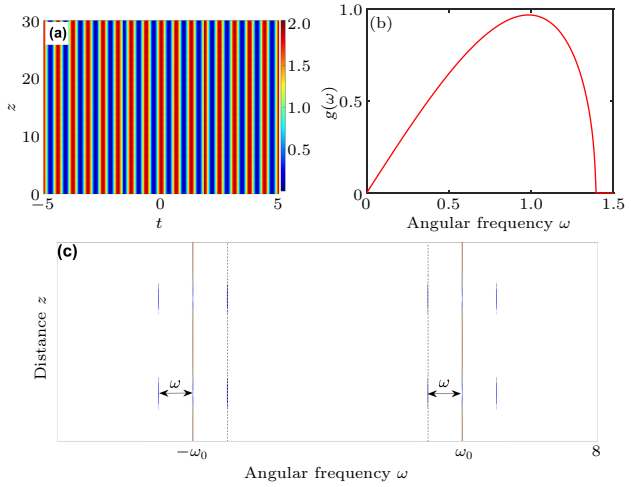


Fig. 1. (a) Temporal evolutions of the total intensity $|\psi_0|^2$ with $\omega_0 = 5$. (b) MI gain spectrum profile for Eq. (1) at $\omega_0 = 4$. (c) Schematic representation of MI produced by dual-wavelength pump (dashed vertical lines label the first-order sidebands, ω stands for modulation frequency). Here, $P = 1$.

3. Multi-wave truncation model and heteroclinic structure

Although linear stability analysis can be used to predict the initial stage of instability, it could not provide any further insight into the long-term behavior of the system. However, important insights into dynamics can be gained by using the MWT method. Here, only dual-wavelength pumps and their respective ±1 order sidebands are considered, with frequencies $\pm\omega_0$, $\pm\omega_0$–ω, and $\pm\omega_0+\omega$, respectively. The two sets of nonlinear local waves with different frequencies have the same evolution properties except for the different group velocities. Therefore, based on the physical process of dual-wavelength pump propagation, we construct the breather solution of Eq. (1), which has a unique form as follows:

$$\begin{aligned}\psi(z,t) &= u(z,t-z\omega_0)\exp(\mathrm{i}\omega_0 t) \\ &\quad + u(z,t+z\omega_0)\exp(-\mathrm{i}\omega_0 t),\end{aligned} \tag{3a}$$

with

$$\begin{aligned}u(z,t) &= \sqrt{\frac{P}{2}}\Big[\sqrt{1-\eta}\exp(\mathrm{i}\varphi_0) + \sqrt{\frac{\eta}{2}}\exp(\mathrm{i}\omega t + \mathrm{i}\varphi_1) \\ &\quad + \sqrt{\frac{\eta}{2}}\exp(-\mathrm{i}\omega t + \mathrm{i}\varphi_{-1})\Big],\end{aligned} \tag{3b}$$

where Eq. (3a) describes the dynamic process of cross-phase modulation of dual-wavelength pumps by a simple expression. $u(z,t)$ is the wave function obtained by dual-wavelength pumps under the relatively stationary coordinate of their propagation when the group velocity is zero. $\varphi_0(z)$ and $\varphi_{\pm1}(z)$ are the pump and sidebands phases, and $\eta(z)$ is the total power of the first-order sidebands. Assuming the total power fraction of the field in Eq. (1) is equal to 1, it is convenient to define the sidebands fraction η and pump fraction $1-\eta$. ω_c is the critical frequency, which is the crossed point of the stable branch of $\Delta\phi_e = \pi/2$ (black solid line) and the unstable branch of $\eta_e = 1$ (red dash line) as shown in Fig. 2(a). The frequency ω is henceforth limited to $\omega_c < \omega < \omega_{\max}$ to effectively prevent higher-order MI from occurring. Substituting Eq. (3) into Eq. (1), the Hamiltonian form of the nonlinear wave evolution is obtained as follows:

$$\dot{\eta} = -\frac{\partial H}{\partial \Delta\phi}, \quad \Delta\dot{\phi} = \frac{\partial H}{\partial \eta}, \tag{4a}$$

$$\begin{aligned}H &= \frac{1}{2}\eta[-\omega^2 + PQ(z)] + \frac{1}{2}P\eta(1-\eta)\cos(2\Delta\phi)Q(z) \\ &\quad - \frac{1}{4}P\eta^2 S(z),\end{aligned} \tag{4b}$$

where the dot denotes derivation with respect to z and $\Delta\phi = (\varphi_1 + \varphi_2 - 2\varphi_0)/2$ is the effective phase. $Q(z) = 1 + 2\cos(2\omega\omega_0 z)$ and $S(z) = (3/2) + 4\cos(2\omega\omega_0 z) - \cos(4\omega\omega_0 z)$. It is evident that the Hamiltonian function H exhibits periodic behavior, indicating that it is not a conserved quantity. As a result, it is unable to construct a phase space

diagram for H. To resolve the problem, we take the average of H. The average Hamiltonian $\bar{H}$ reads

$$\bar{H} = -\frac{1}{2}\eta\omega^2 + \frac{1}{2}P\eta + \frac{1}{2}P\eta(1-\eta)\cos(2\Delta\phi) - \frac{3}{8}P\eta^2. \quad (5)$$

The average Hamiltonian $\bar{H}$ can be described as contours on the $(\Delta\phi, \eta)$ phase plane as shown in Fig. 2(b), where all possible dynamic trajectories of MI at frequency ω are given. Obviously, the contours of $\bar{H}$ have a heteroclinic structure, and there is a separatrix (see the closed black line in Fig. 2(b)) that divides the phase plane into regions of inner and outer orbits. The evolution of MI can be comprehensively analyzed from the phase plane portrait of $\bar{H}$.

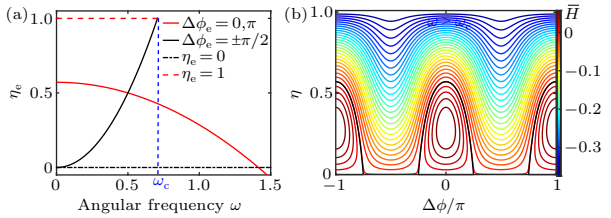


Fig. 2. (a) Stationary sideband fraction η_e of stable (solid lines) and unstable (dash and dash-dotted lines) branches versus ω beyond ω_c. (b) Average Hamiltonian contours on the phase plane $(\Delta\phi, \eta)$ for $\omega = 1$. The black curve is heteroclinic separatrix with $\eta_e = 1$, dividing the phase plane into two different domains. Here, $P = 1$, $\omega_0 = 4$ and $\omega_c = (P/2)^{1/2}$.

Equation (5) has four groups of stationary points $(\Delta\phi_e, \eta_e)$ (solutions of $d\eta/dz = d\Delta\phi/dz = 0$) corresponding to four eigenmodes. Figure 2(a) shows the bifurcation diagram, i.e., the value η_e of the stationary points versus frequency ω. In the gain range that we have studied, only heteroclinic separatrix with stationary points $\eta_e = 0$ is considered. In this case, the heteroclinic structure follows the well-known structure of the integrable NLSE.[25,34] Hence, we have disregarded the two stationary points of $(\Delta\phi_e, \eta_e) = [\pi/2, 2\omega^2/P]$ and $(\Delta\phi_e, \eta_e) = [0.5\cos^{-1}(-(\omega^2/P) - 0.5), 1]$. There are only two stationary points directly related to the heteroclinic structure here.

One of the group stationary points of $(\Delta\phi_e, \eta_e) = [0$ or π, $-(2\omega^2/7P) + (4/7)]$ corresponds to the maxima of $\bar{H}$. This eigenmode is stable because the contour of $\bar{H}$ shrinks to the point $(\Delta\phi_e, \eta_e)$ when the Hamiltonian $\bar{H}$ reaches its extreme value. The red solid line in Fig. 2(a) gives the relationship between the sideband fraction η_e and modulation frequency ω. Only if the input condition satisfies $\bar{H}\ (\Delta\phi_e, \eta_e) = (\omega^4/14P) - (\omega^2/2) + (2P/7)$, it will evolve asymptotically toward such eigenmode.

Another group stationary points of $(\Delta\phi_e, \eta_e) = [\pm 0.5\cos^{-1}(-(\omega^2/P) - 1), 0]$ suggest unstable eigenmodes and turn out to be the bottom vertexes of the contour $\bar{H}$ in the frequency range of $\omega < \omega_{max}$, which agrees with the MI gain bandwidth from linear stability analysis. It is worth noting that the contour of $\bar{H} = 0$ composes the heteroclinic separatrix, on which the latticed ABs can be excited. Strictly speaking, only if the input condition satisfies $\bar{H}(\Delta\phi_0, \eta_0) = 0$, the nonlinear wave evolution pattern of Eq. (3) belongs to the latticed ABs. However, the interaction between the dual-wavelength pumps induced by the cross-phase modulation, results in the generation of extra optical waves. As a consequence, the latticed ABs cannot be excited and can only obtain FPU recurrence evolution, as shown in Fig. 3(a).

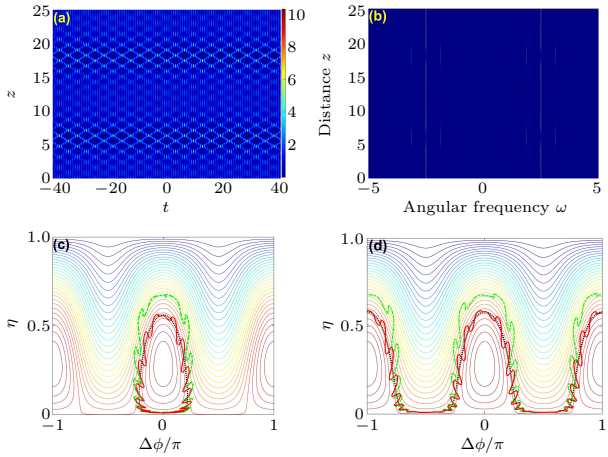


Fig. 3. Latticed ABs recurrent evolution through numerical integration of Eq. (1) with $\eta_0 = 0.01$. Panels (a) and (b) show the temporal and spectral evolutions of the total intensity $|\psi(z,t)|^2$. Panels (c) and (d) show the corresponding projections of Eq. (1) (green dash-dotted line), Eq. (4a) (red solid line), and Eq. (5) (black dotted lines) on the phase plane $(\Delta\phi, \eta)$ for (c) $\Delta\phi_0 = 0$ and (d) $\Delta\phi_0 = \pi/2$. Here, $P = 1$, $\omega_0 = 4$, and $\omega = 1$.

4. Latticed-Fermi–Pastel–Ulam recurrences

The bifurcations illustrated in Fig. 2 have a profound influence on the long-term evolution of the nonlinear wave in Eq. (1). In order to show this, we numerically integrate Eq. (1) by taking the modulated dual-wavelength pumps as the initial condition

$$\psi(0,t) = \sqrt{2P}\cos(\omega_0 t)\Big[\sqrt{1-\eta_0} + \sqrt{\eta_0/2}\exp(i\omega t + i\Delta\phi_0) + \sqrt{\eta_0/2}\exp(-i\omega t + i\Delta\phi_0)\Big], \quad (6)$$

where η_0 is the initial sidebands fraction, and $\Delta\phi_0$ is the overall initial effective phase $\Delta\phi_0 = \Delta\phi(0)$.

Next, we illustrate the nonlinear wave evolutions and dynamic trajectories inside and outside the heteroclinic separatrix for $\omega > \omega_c$. Because there is no essential difference in the latticed ABs patterns we obtained under two different initial effective phase conditions, only one of the recurrent regimes is shown in Figs. 3(a) and 3(b), where $\Delta\phi_0 = 0$. However, the projection of Eq. (1) evolved onto the phase space reveals very different behaviors for the two initial effective phase conditions. Figures 3(c) and 3(d) depict their dynamic trajectories with the initial phases of $\Delta\phi_0 = 0$ and $\Delta\phi_0 = \pi/2$. All three trajectories are obtained in the numerical results from Eq. (1) (green dash-dotted line), Eq. (4a) (red solid line) and Eq. (5) (black dotted lines), respectively. One can see that the numerical results by Eq. (4a) are significantly different from those

by Eq. (5) induced by neglecting the four-wave mixing process. The dynamic trajectory obtained by integrating Eq. (4a) oscillates with the evolution of z. Meanwhile, Eqs. (4a) and (1) also exhibit deviations due to the neglect of higher-order sidebands.

Theoretically, the above Figs. 3(a) and 3(b) behaviors correspond to different spatiotemporal evolution. To prove it, under such an input condition of Eq. (6), we utilize the split-step Fourier transform method to implement the numerical integration of Eq. (1). Then, we filter the spectrum of $\psi(z,t)$ to obtain the optical-wave evolution of $u(z,t)$. Actually, in order to extract $u(z,t)$ from Eq. (3), we perform a coordinate transformation on it. Finally, we obtain the unshifted and staggered FPU recurrences under two initial phase conditions, as shown in Fig. 4. Figure 4(a) shows that the FPU recurrence drift is caused by the Kerr nonlinear effect. This phenomenon arises from the acute variation in the nonlinear refractive index of the medium under the nonlinear superposition of two optical intensities. Furthermore, the two patterns shown in Fig. 4 correspond to the orbit in Figs. 3(c) and 3(d), respectively.

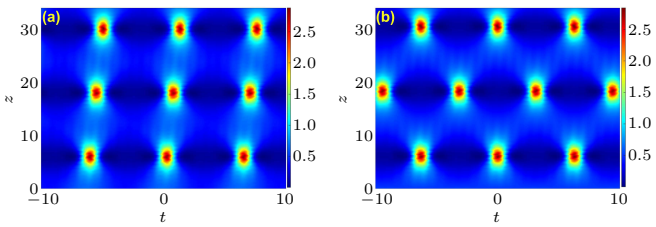


Fig. 4. Two types of FPU evolutions through numerical integration of Eq. (1) with initial effective phases: $\Delta\phi_0 = 0$ (unshifted) (a) and $\Delta\phi_0 = \pi/2$ (staggered) (b). The above temporal evolution of the intensity is $|u(z,t)|^2$. All parameters are the same as in Fig. 3.

5. Conclusion

We study numerically the nonlinear stage of the modulation instability of the dual-wavelength pumped in the framework of the nonlinear Schrödinger equation. It is interesting to note that, NLSE has an approximate stationary solution which is linearly superimposed by two plane wave solutions. The existence condition of the solution is given and confirmed by numerical simulation. Dramatically, we show that the latticed-FPU recurrences can be excited on the modulated-wave background in NLSE. These results further enrich the types of nonlinear local waves. From our work, we hope to further broaden and deepen the understanding of MI.

Acknowledgments

Project supported by the National Natural Science Foundation of China (NSFC) (Grant No. 12004309), the Shaanxi Fundamental Science Research Project for Mathematics and Physics (Grant No. 22JSQ036), and the Scientific Research Program funded by Shaanxi Provincial Education Department (Grant No. 20JK0947).

References

[1] Abdullaev F K, Baizakov B B, Darmanyan S A, Konotop V V and Salerno M 2001 *Phys. Rev. A* **64** 043606
[2] Zhao L C 2018 *Phys. Rev. E* **97** 062201
[3] Benjamin T B and Feir J E 1967 *J. Fluid Mech.* **27** 417
[4] Tai K, Hasegawa A and Tomita A 1986 *Phys. Rev. Lett.* **56** 135
[5] Taniuti T and Washimi H 1968 *Phys. Rev. Lett.* **21** 209
[6] Zakharov V E and Ostrovsky L A 2009 *Physica D* **238** 540
[7] Hammani K, Wetzel B, Kibler B, Fatome J, Finot C, Millot G, Akhmediev N and Dudley J 2011 *Opt. Lett.* **36** 2140
[8] Akhmediev N and Korneev V 1986 *Theor. Math. Phys.* **69** 1089
[9] Frisquet B, Kibler B and Millot G 2013 *Phys. Rev. X* **3** 041032
[10] Mussot A, Kudlinski A, Droques M, Szriftgiser P and Akhmediev N 2014 *Phys. Rev. X* **4** 011054
[11] Kimmoun O, Hsu H C, Branger H, Li M S, Chen Y Y, Kharif C, Onorato M, Kelleher E J R, Kibler B, Akhmediev N and Chabchoub A 2016 *Sci. Rep.* **6** srep28516
[12] Pierangeli D, Flammini M, Zhang L, Marcucci G, Agranat A, Grinevich P, Santini P, Conti C and DelRe E 2018 *Phys. Rev. X* **8** 041017
[13] Kibler B, Chabchoub A, Gelash A, Akhmediev N and Zakharov V E 2015 *Phys. Rev. X* **5** 041026
[14] Liu C and Akhmediev N 2019 *Phys. Rev. E* **100** 062201
[15] Liu C, Yang Z Y and Yang W L 2018 *Chaos* **28** 083110
[16] Zhao L C, Ling L and Yang Z Y 2018 *Phys. Rev. E* **97** 022218
[17] Kibler B, Fatome J, Finot C, Millot G, Genty G, Wetzel B, Akhmediev N, Dias F and Dudley J M 2012 *Sci. Rep.* **2** 463
[18] Solli D R, Ropers C, Koonath P and Jalali B 2007 *Nature* **450** 1054
[19] Akhmediev N, Soto-Crespo J M and Ankiewicz A 2009 *Phys. Lett. A* **373** 2137
[20] Liu C, Yang Z, Zhao L, Xin G and Yang W 2014 *Opt. Lett.* **39** 1057
[21] Zhao L C, Duan L, Gao P and Yang Z Y 2019 *Europhys. Lett.* **125** 40003
[22] Yao X, Liu C, Yang Z Y and Yang W L 2022 *Phys. Rev. Res.* **4** 013246
[23] Yao X K, Yang Z Y and Yang W L 2021 *Nonlinear Dyn.* **103** 1035
[24] Herbst B M, Ablowitz M J and Ryan E 1991 *Comput. Phys. Commun.* **65** 137
[25] Mussot A, Naveau C, Conforti M, Kudlinski A, Copie F, Szriftgiser P and Trillo S 2018 *Nat. Photonics* **12** 303
[26] Sheveleva A, Colman P, Dudley J M and Finot C 2023 *Opt. Commun.* **538** 129472
[27] Conforti M, Mussot A, Kudlinski A, Nodari S, Dujardin G, De Biévre S, Armaroli A and Trillo A 2016 *Phys. Rev. Lett.* **117** 013901
[28] De Angelis C, Santagiustina M and Trillo S 1995 *Phys. Rev. A* **51** 774
[29] Mussot A, Conforti M, Trillo S, Copie F and Kudlinski A 2018 *Adv. Opt. Photonics* **10** 1
[30] Deng Z, Zhang J, Fan D and Zhang L 2022 *New J. Phys.* **24** 063018
[31] Bessin F, Naveau C, Conforti M, Kudlinski A, Szriftgiser P and Mussot A 2022 *Commun. Phys.* **5** 6
[32] Vanderhaegen G, Szriftgiser P, Kudlinski A, Armaroli A, Conforti M, Mussot A and Trillo S 2023 *Phys. Rev. A* **108** 033507
[33] Haelterman M, Trillo S and Wabnitz S 1992 *Opt. Lett.* **17** 745
[34] Trillo S and Wabnitz S 1991 *Opt. Lett.* **16** 986
[35] Lan Y, Zhao L C and Luo X 2019 *Commun. Nonlinear Sci. Numer. Simul.* **70** 334
[36] Zhao L C, Ling L, Qi J W, Yang Z Y and Yang Z Y 2017 *Commun. Nonlinear Sci. Numer. Simul.* **49** 39
[37] Agafontsev D S and Zakharov V E 2016 *Nonlinearity* **29** 3551
[38] Luo Z C, Luo A P, Xu W C, Liu J R and Yin H S 2010 *Appl. Phys. B* **100** 811
[39] Trillo S, Wabnitz S and Kennedy T A B 1994 *Phys. Rev. A* **50** 1732